Desalination and Water Treatment
www.deswater.com

doi: 10.5004/dwt.2018.23246

136 (2018) 138–149
December

Effects of aluminum (Al^{3+}) on sludge digestion and biofilm development in attached growth batch reactors using tire-derived rubber as a media

Iqra Sharafat[a,†], Dania Khalid Saeed[a,b,†], Zargona Zafar[a], Naeem Ali[a,*]

[a]*Department of Microbiology, Quaid-I-Azam University, 45320, Islamabad, Pakistan, Tel. +92 051 90643194; emails: naeemali2611@gmail.com, naeemali95@gmail.com (N. Ali), sharafatiqra@yahoo.com (I. Sharafat), dksaeed@mail.com (D.K. Saeed), zargonazafar@gmail.com (Z. Zafar)*
[b]*Department of Pathology and Laboratory Medicine, Agha Khan University, Karachi, Pakistan*

Received 6 September 2017; Accepted 4 October 2018

ABSTRACT

Effects of varying concentrations of aluminum (Al^{3+}) on sludge digestion and biofilm development on waste tire rubber were determined in attached growth batch reactors (AGBR) for 30 d under anoxic conditions. The strategy was bi-pronged where performance of the reactors was measured through activated sludge liquor digestibility and nitrogen removal viz. chemical oxygen demand (COD), NO_2^--N/NO_3^--N, respectively. Overall, increase in Al^{3+} concentration (0–6.5 mg/L) resulted a decrease (7.33%) in bacterial density. Biochemical characterization of the bacterial isolates confirmed that most of them were gram negative. Moreover, fluorescence in situ hybridization (FISH) coupled with confocal laser scanning microscopy (CLSM) and spatial distribution analysis of the biofilms indicated presence of beta and gamma proteobacteria. Bacterial population densities decreased with increasing levels of Al^{3+}. Additionally, sludge digestibility decreased in the reactors as high levels of COD (438 mg/L) and volatile fatty acids (VFA; 350 mg/L) were recorded at 6.5 mg/L of Al^{3+}. Ammonium nitrogen (NH_4^+-N) transformation measured as NO_3^--N and NO_2^--N indicated an overall decrease in both the inorganic forms of nitrogen with highest elimination rate of NO_2^- at 4.5 mg/L Al^{3+}, whereas, lowest was recorded at 2.5 mg/L Al^{3+}. Generally, the study revealed a limiting effect of Al^{3+} concentration at specific levels on sludge digestibility, bacterial density, diversity and metabolism in the AGBR.

Keywords: Aluminum (Al^{3+}); Biofilms; Wastewater treatment; Community composition; Tire-derived rubber; Fluorescence in situ hybridization (FISH); Confocal laser scanning microscopy (CLSM)

1. Introduction

Ubiquity of biofilms as recalcitrant three-dimensional matrices on biotic and abiotic surfaces translates into a unique conundrum. The inherent bio-catalysis of complex compounds and production of secondary metabolites by biofilms has been exploited to develop environmentally sustainable and novel technologies for waste water treatment and energy production [1,2]. Whereas, great economic losses have been incurred due to the unmitigated growth of biofilms on surfaces and membrane filters presenting a compounding challenge that needs to be circumvented. The preference of bacteria to grow on attached rather than in the suspended phase [3] is contributed by a complex interaction between the bacteria and surface chemistry of support material [4]. The tendency of bacteria to attach to surfaces has been extensively studied with respect to microbiologically induced corrosion or biofouling of piping surfaces employed in water, waste water, oil and gas distribution networks, bioreactor membranes or other propagating surfaces [5]. In order to promote environmentally sustainable technologies, it is imperative to address the issue of low cost of treatment options by focusing on usage of cheap biofilm support materials. Billions of used tires are stockpiled annually owing to unavailability of their alternate applications. In this context, waste tire-derived rubber has been viewed as

* Corresponding author.
† Authors contributed equally.

an alternative to different costly materials in attached growth biofilm reactors due to its good surface area, less toxicity to microorganisms and size distribution. Previously, a number of bioreactors, such as trickling filters and hybrid sludge biofilm bed reactor using tire-derived rubber as support, have been run with considerable treatment efficiencies [6–9]. Still, detailed understanding of the factors influencing biofilm structure and growth is imperative to harness the potential of the said bioreactors.

Typically, aluminum ions and poly alum compounds have been recommended as effective coagulants for removal of chemical oxygen demand (COD) and biological oxygen demand (BOD) in wastewater treatment [10]. Iron and aluminum hydroxide coatings on filtering materials such as sand have also been reported to effectively remove fecal coliforms from water [8] and achieved a reduction of 4 log in the bacterial count after passing waste water through sand columns coated with iron and aluminum hydroxide. Similarly, Zhu et al. [11] indicated that aluminum sulfate removed color and COD by 72% and 90%, respectively.

In vitro studies to evaluate the effect of different parameters such as oxygen, carbon dioxide, nutrients on biofilm formation rely on the use of biofilm reactors that can be either batch reactor or open systems [12–14]. The advent of scanning and transmission electron microscopy enabled an in-depth exploration and higher resolution of biofilms to be studied [15]. Bacterial density and biochemical identification have been conducted using conventional culture based methods. However, these methods have their limitations such as inability to identify non-culturable bacteria. Two major thrusts in the previous two decades have impacted our understanding of biofilms including molecular methods such as fluorescence in situ hybridization (FISH) and confocal laser scanning microscopy (CLSM) [16,17]. Herten et al. [18] quantified *Staphylococcus aureus* biofilm formation on vascular graft surfaces by using conventional culture based techniques to determine colony forming units and validated their findings qualitatively using scanning electron microscopy (SEM). Fish et al. [19] characterized the physical composition and microbial community composition of biofilms of their full scale model water distribution system using fluorescent CLSM and digital image analysis (DIA). Similarly, Sharafat et al. [20] quantified microbial density in biofilms developed on waste tire rubber with FISH and CLSM.

Despite established role of aluminum as a coagulant, the role of these flocculating agents on biofilm development dynamics and floc stability has not been extensively studied specifically with regards to Al^{3+} [21–23]. A gap exists in our understanding of aluminum's role in terms of overall microbial diversity in biological wastewater treatment and water sanitation systems. Thus, this study evaluated the effects of varying concentrations of aluminum on biofilm development and associated bacterial densities on tire-derived rubber as a cheap support material through conventional and molecular based techniques such as FISH and CLSM. Besides, the effect of varying concentrations of aluminum on reactors performance was monitored in terms of waste water's sludge digestibility along with nitrification rates.

2. Materials and methods

2.1. Development of biofilms on tire-derived rubber support

2.1.1. Sampling

Activated sludge was collected from municipal waste water treatment plant located in Islamabad, Pakistan, in sterilized plastic containers. Sample was transported within an hour to laboratory in cold sampling box and stored at 4°C prior to inoculation into the reactors on the same day.

2.1.2. Set up and operation of attached growth batch bioreactors

Strips of waste tire-derived rubber (TDR) (surface area: 93.48 cm^3) were cut and vertically aligned in four attached growth batch reactors (AGBR) in duplicate, with a total capacity of 4 L each and working volume of 3 L. The TDR strips incorporated in the reactors were of a passenger car and they were suspended inside the reactors with an iron wire such that three fourth was covered with waste activated sludge. The composition of the TDR included crumb rubber (70%), fibers and scrap (13%) and steel (17%) [24]. Composition of the medium used within each reactor was as follows: 2 L activated sludge, 1 L minimal salt media (64 g Na_2HPO_4, 15 g KH_2PO_4, 2.5 g NaCl, 5.0 g NH_4Cl, 1 M Mg_2SO_4, 20% glucose and 1 M $CaCl_2$), 5 mL trace elements (10 mg $ZnSO_4.7H_2O$, 3 mg $MnSO_4$, 1 mg $CoCl_2.6H_2O$, 20 mg $NiCl_2.6H_2O$, 30 mg $Na_2Mo.2H_2O$, 30 mg H_3BO_3, 1 mg $CuCl_2.2H_2O$, 1 mg $CuSO_4$), 5 g starch and 5 g technical agar (Oxoid). The characterization of the wastewater from this facility, according to European Standards was as follows: HRT: 7 d, MLSS: 3,000–3,500 mg/L, TSS: influents; 230–235 mg/L, effluents: 35 mg/L, BOD: 190–200 mg/L, COD (Influent): ≈700 mg/L, COD (effluent): 150 mg/L. The batch reactors were covered with black paper to prevent any algal growth and incubated at 30°C ± 2°C. After incubation of 2 d as an acclimatization period, three reactors were dosed with three different concentrations of $AlCl_3$ (2.5, 4.5 and 6.5 mg/L) and homogenized with stirrers, whereas, control reactor received no aluminum. The reactors were incubated under anoxic condition at 30°C for a period of 30 d. Mechanical stirring was carried out with sterile stainless stirrers periodically to ensure appropriate oxygen diffusion and homogeneity of the contents in the reactors.

2.2. Physico-chemical characterization of activated sludge liquor in reactors

Sludge digestion in the reactors was measured in terms of different physicochemical parameters. COD (mg/L), VFA (mg/L) and alkalinity (mEq/L) of sludge were measured initially and at final stage (after 30 d of treatment), using COD commercial kits (Merck, Germany, detection range; 25–2,500 mg/L) and three point titration method [25], respectively. In addition, NO_3-N and NO_2-N of the activated sludge were measured, using APHA 4500 NO_3-N and APHA 4500 NO_2–N methods (Standard Methods, 2005) [26], respectively. The pH of the samples was determined periodically using "Digital Sartorius (pp 15) pH meter". Dissolved oxygen (DO) was monitored with "Crison OXI45+ DO meter" that contained

5120 electrode. The electrode of the meter was washed three times with distilled water before analyzing each sample.

2.3. Evaluation of bacterial density in biofilms of tire-derived rubber

Biofilms developed on TDR, under the influence of different aluminum concentrations after enrichment culture technique, were gently washed with PBS to remove any planktonic microorganism. The biofilm were scraped off from 1 cm^2 sections of the support using sterile surgical blade. The cuttings were then sonicated at 1–2 kHz for 3 min. Bacterial biofilm density on the tire-derived support surface was determined on the basis of CFU/mL cm^2 using heterotrophic plate count method on nutrient agar plates in triplicate and analyzed statistically with t-test using Microsoft excel 2015. Pure cultures of bacteria obtained on nutrient agar plates were biochemically characterized and identified using standard procedures and following Bergey's Manual of Determinative Bacteriology [27].

2.4. Scanning electron microscopy of biofilm on TDR

To visualize the surface morphology of biofilms on TDR, SEM of the biofilms on TDR from attached growth batch reactors (control [0 mg/L] and 6.5 mg/LAl^{3+}) was carried out. Small sections of fixed biofilm samples on TDR were mounted on copper stubs and sputter coated with gold layer. Then vacuum was generated by applying high voltage in ion sputtering device (JFC-1500, auto coater, JEOL, Tokyo, Japan) for gold deposition on biofilms. 25 mA current for approximately 50 s was used for plasma generation and subsequent gold coating on the samples. Gold coated samples were then placed under the column in chamber and finally the micrographs were observed under SEM (JSM-6490A, JEOL) at different magnification intensities starting from X100 to X20,000 and recorded.

2.5. Microbial community analysis of biofilms by FISH and confocal laser scanning microscope

To check the specificity of fluorescent probes and for hybridization optimization, bacterial strains, that is, *Bacillus subtilis*; accession no. KJ600795 and *Pseudomonas aeruginosa* ATCC ® 9027™) were applied as positive reference cells for β and ϒ communities of proteobacteria in the upper wells of the slides (Figs. S1 and S2). Biofilms on TDR were washed with sterile distilled water to remove planktonic microorganisms. The biofilms were transferred from 1 cm^2 surface area of the support media to 10 well Teflon coated glass slides followed by fixation with 4% paraformaldehyde (PFA) for 2 h (–20°C) according to protocols described by Manz et al. [28], with slight modifications for non-disruptive fixation of bacteria. After washing samples with PBS (pH 7.2), the samples were successively dehydrated using 50%, 80% and 100% ethanol and stored at room temperature before further processing. 18 μl of hybridization buffer (20mM Tris HCl (pH 7.2), 0.9 M NaCl), 0.01% sodium dodecyl sulfide (SDS), 35% formamide (deionized) and 2 μL of 5′ end fluorescently labeled 5, 6 FAM (FLUOS derivatives; amine reactive succinimidyl esters of carboxyfluorescein) oligonucleotide probes were pipetted out into each well. 2 μL of corresponding unlabeled competitor probes were also added to ensure specific binding. Fluorescent labeled probes and their corresponding unlabeled competitors, used in this study, were obtained from α-oligos (Montreal, Canada). Details of fluorescent probes (Gam42a and Beta-42a) are mentioned in Table 1. After incubating slides for 90 min in hybridization chamber at 46°C, the slides were washed with prewarmed washing buffer (20 mM Tris/HCl, 0.01% SDS, 5 M NaCl), rinsed with distilled water, dried and mounted in Citifluor. Prepared hybridized slides were viewed under FluoView™ (Fv1000) confocal laser scanning microscope equipped with multi argon ion lasers (409–552 nm) and optical sections were collected under Kalman filtration mode. Multiple field of views (FOV) were selected containing maximum cells for image acquisition.

Table 1
Sequences and specificity of 5′ end 5,6-FAM labeled 16S rRNA oligonucleotide probes

No.	Probe (Full name)[a]	Specificity	Binding position[b] (bp)	5′-End labeled (5,6-FAM) probe sequence	References
1	EUB338- I (S-D-Bact-0338-a-A-18)	16S rRNA, majority of bacteria	338–355	GCTGCCTCCCGTAGGAGT	[30]
2	EUB338- II (S-*-BactP-0338-a-A-18)	16S rRNA, bacteria not targeted by EUB338-I	338–355	GCAGCCACCCGTAGG TGT	[29]
3	EUB338- III (S-*-BactV-0338-a-A-18)	16S rRNA, bacteria not covered by EUB338-I and EUB338-II, *Verrucomicrobiales*	338–355	GCTGCCACCCGTAGGTGT	[29]
4	Bet42a[c] (L-C-bProt-1027-a-A-17)	β-Proteobacteria	1,027–1,043	GCCTTCCCACTTCGTTT	[28]
5	Gam42a[c] (L-C-gProt-1027-a-A-17)	γ-Proteobacteria	1,027–1,043	GCCTTCCCACATCGTTT	[28]

[a]Full name of 16S rRNA gene-targeted oligonucleotide probe(s) is based on the nomenclature of Alm et al. [31].
[b]Probe binding positions according to *E. coli* 16S rRNA gene numbering [32].
[c]Competitor probes of Bet42a and Gam42a were also added to the hybridization buffer as unlabeled oligonucleotide probes in equimolar amounts as the labeled probes to enhance the hybridization specificity [28].

The images were reserved in TIFF format for further processing. Quantification of the microbial populations (average of three images) was carried out using daime (DIA in microbial ecology) software [29]. Only those results were included in analysis that showed significant intensity of signals with the target cells. The image analysis provided us information on parameters, that is, cell numbers, bio-volume fraction and biomass (area of cells). Upper and lower cut offs were chosen to avoid objects to avoid objects (too small or large) to be bacteria during image processing.

3. Results

3.1. Physicochemical profile of activated sludge in AGBR under varying concentrations of Al^{3+}

Varying concentrations of Al^{3+} proved to have a significant effect on the overall digestion of sludge in the AGBR in 30 d. COD (mg/L) of raw sludge was reduced when treated with different concentrations of Al^{3+} compared with untreated sample. Maximum removal of COD was 28.68% at 2.5 mg/L of Al^{3+} followed by 27.11% and 13.95% at 4.5 and 6.5 mg/L Al^{3+}, respectively (Fig. 1).

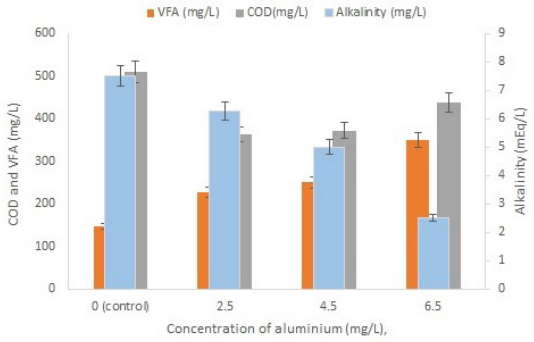

Fig. 1. Variation in concentration of COD, volatile fatty acid (VFA) and alkalinity of sludge in attached growth batch reactors after 30 d of treatment (raw sludge characteristics: COD; 700 mg/L, VFA; 27.5 mg/L, alkalinity; 9.5 mg/L).

VFA and alkalinity of the activated sludge seed were determined to be around 9.5 mg/L and 27.5 mEq/L, respectively. After incubation in AGBR, alkalinity of activated sludge decreased with increase in Al^{3+} concentration in the reactors. Under control condition (Al^{+3} = 0 mg/L) it remained 7.5 mEq/L whereas, minimum alkalinity of 2.5 mEq/L was observed at 6.5 mg/L of Al^{3+} (Fig. 1). Contrarily, minimum level (147.5 mg/L) of VFA was observed under control condition that increased with increasing concentration in the following order: 227.5, 250 and 350 mg/L for 2.5, 4.5 and 6.5 mg/L of Al^{3+}, respectively (Fig. 1, Table S1).

The concentration (mg/L) of nitrite nitrogen in the reactor serving as control (0 mg/L Al^{3+}) and those dosed with a range of Al^{3+} concentrations, that is, 2.5, 4.5 and 6.5 mg/L were as follows: 182.0, 39.0, 47.0 and 59.0 mg/L, respectively, at the first week of operation. Percentage change for NO_2^- was highest, that is, 77% (96 mg/L) at 2.5 mg/L followed by control, 4.5 and then 6.5 mg/L of Al^{3+} (Fig. 2). Trend for NO_2^- (mg/L) followed a linear decrease in the first 3 weeks of incubation for untreated sludge (0 mg/L Al^{3+}). Whereas, under treated conditions an increase in NO_2^- (mg/L) till midweek with a linear decrease in the proceeding next was observed. Difference in the rate of percentage change of nitrite concentration between consecutive weeks for treated reactors followed a decreasing trend with increasing concentration of Al^{3+}. The final concentrations of nitrite in the reactors on 30th day were 28.05%, 21.13% and 14.91%, for 2.5, 4.5 and 6.5 mg/L of Al^{+3}, respectively.

Nitrates concentration decreased with time specifically under experimental (treated) conditions. Initial reading for nitrate concentration in treated and control sludge samples (2.5, 4.5 and 6.5 mg/L of Al^{3+}) were 168.8, 219.7, 249.2 and 216.1 mg/L, which decreased to 163.7, 148.4, 114.2 and 115.8 mg/L, respectively, in the third week. The decreasing trends in nitrates reduction rates were 54.17%, 46.41%, 32.40% and 30.2% at 4.5, 6.5, 2.5 and 0 mg/L of Al^{+3}, respectively (Fig. 2; Table S2). Under control condition, there was 22.39% increase in nitrate concentration by the second week, followed with a decline in the third week from 206.6 to 163.7 mg/L, that is, a percentage decrease of 20.76%.

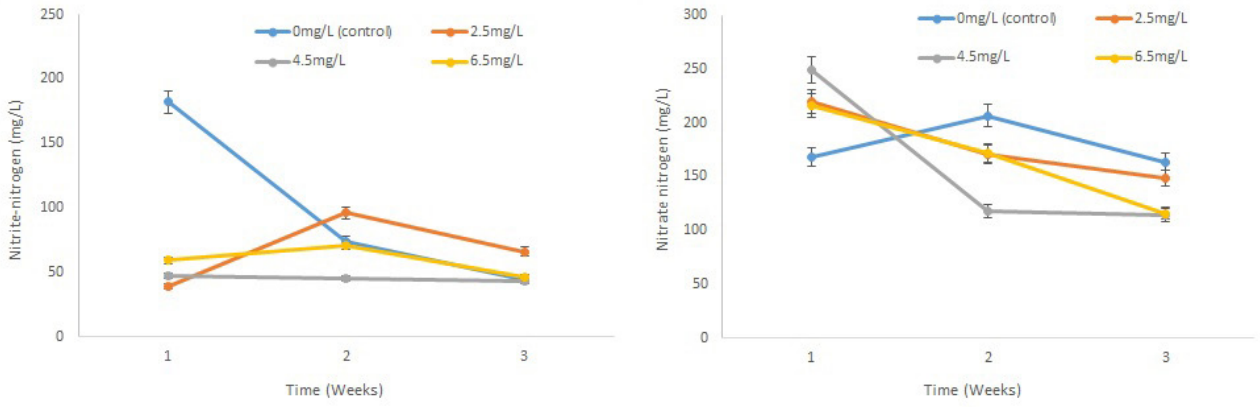

Fig. 2. Transformation rate of nitrogen in terms of NO_2^- (mg/L) and NO_3^- (mg/L) in the attached growth batch reactors treated at different concentrations of Al^{3+} (2.5, 4.5 and 6.5 mg/L) over a period of 4 weeks. Time points: 1 = 7th day, 2 = 15th day, 3 = 30th day.

3.2. Influence of aluminum (mg/L) on bacterial density (CFU/mL cm^2) in biofilms

Different concentrations of Al^{3+} (mg/L) proved to have insignificant (ANOVA [$p > 0.05$]) limiting effect on bacterial growth in biofilm developed on TDR after a period of 30 d (A.1, A.2). Under control condition, bacterial count was 9.05E+09 CFU/mL cm^2. However, it reduced by 91.25% when 2.5 mg/L of Al^{3+} was used in the reactor. Further increase in Al^{3+} (mg/L) proved to be more limiting and bacterial count reduced to 98.65% and 98.58% at 4.5 and 6.5 mg/L of Al^{3+}, respectively (Fig. 3, Table S3). Scanning electron micrographs also demonstrated similar results (Figs. 4 and 5). A total of 13 different bacterial genera were identified on the basis of morphology and biochemical assays (Table S4). Majority of the isolates were gram negative, a typical representation of sludge microflora. Potential bacterial isolates included species of genera: *Pseudomonas*, *Bacillus*, *Enterobacter*, *Serratia*, *Proteus*, *Citrobacter*, *Klebsiella pneumoniae*, *Salmonella*, *Staphylococcus*, *Streptococcus* and *Shigella*.

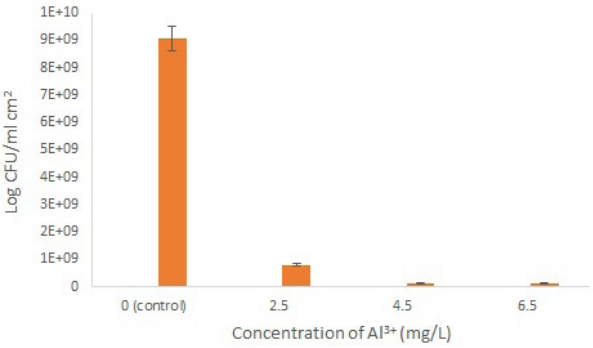

Fig. 3. Culture and physiological based bacterial density (CFU/mL cm^2) in biofilms developed on TDR under the influence of different aluminum concentrations (mg/L).

3.3. FISH-CLSM of biofilms on TDR under the influence of aluminum

Images of biofilms on TDR obtained from FISH and CLSM are given in Fig. 6. EUB probes that targeted the whole eubacterial population showed green fluorescence, whereas beta-proteobacteria and gamma-proteobacteria labeled in separate wells gave red and blue fluorescence, respectively. Moreover, the images depicted aggregating cells and flocs within which overlapping colors, that is, yellow, pink and purple were observed due to the co-aggregation of different bacterial species.

Fig. 7 depicts targeted bacterial population enumerated using daime image analysis software. Eubacterial population exhibited an increasing trend with increasing concentration of Al^{3+} (mg/L) that showed an appreciable decrease when the concentration further increased to 6.5 mg/L. At 100x magnification, the highest average object count in one FOV, that is, 8.02E+02 count of Eubacterial population was recorded in control biofilm, followed by 2.08E+02, 9.20E+01

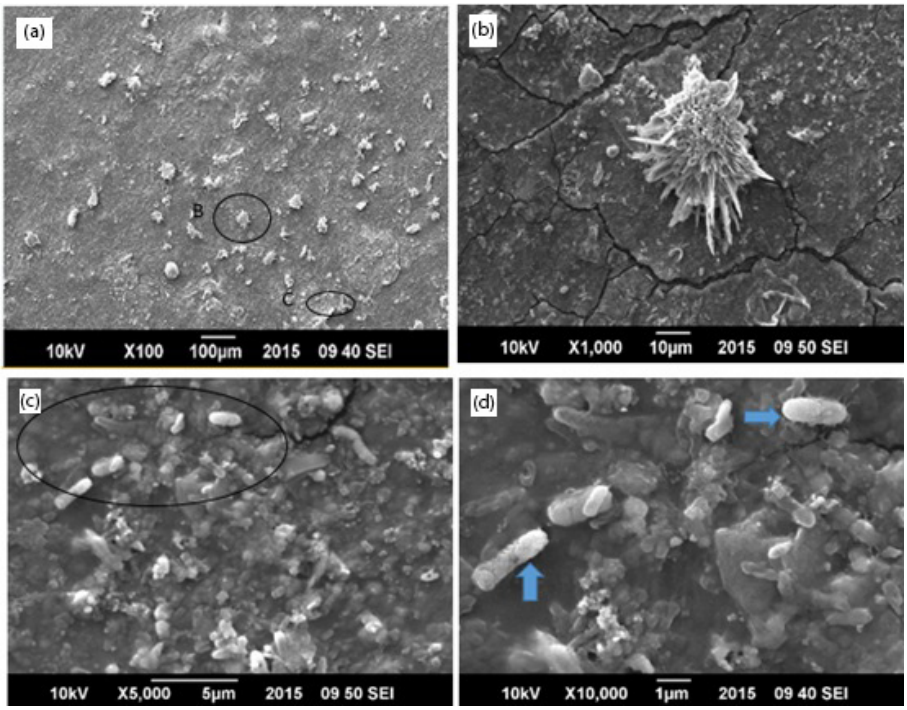

Fig. 4. SEM images showing the formation of biofilms on untreated tire rubber (0 mg/L Al^{3+}). (a) Deposition can be seen at lower magnification of X100. Areas encircled "B" and "C" are further magnified at a resolution of X1,000 and X5,000, respectively. (b) At X1,000, calcite or mineral deposition having astral radiating arms is observed. (c) At X5,000, EPS matrix covering the tire rubber surface is clearly observed. Thick and long elongated rods are observed. The encircled area was magnified to a higher resolution of X10,000 to observe the microbial morphologies clearly. (d) At X10,000 magnification, elongated rods are prominent, there is a thick EPS matrix within which microorganisms are embedded.

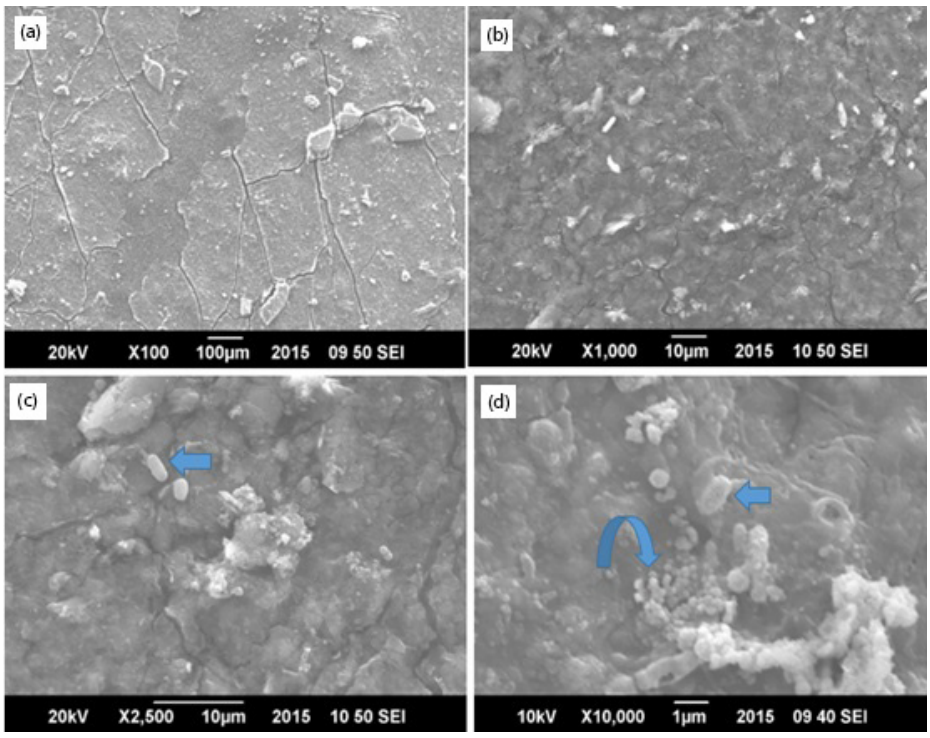

Fig. 5. SEM images of biofilms on tire-derived rubber at 4.5 mg/L Al^{3+}. (a) Cracks and crevices are present as part of the surface topology of the rubber tire. (b) Deposition of minerals can also be seen as dense white structures. (c) and (d) Arrows indicate that cocci and rods are present. Microbial density is less as compared with biofilm from control reactor.

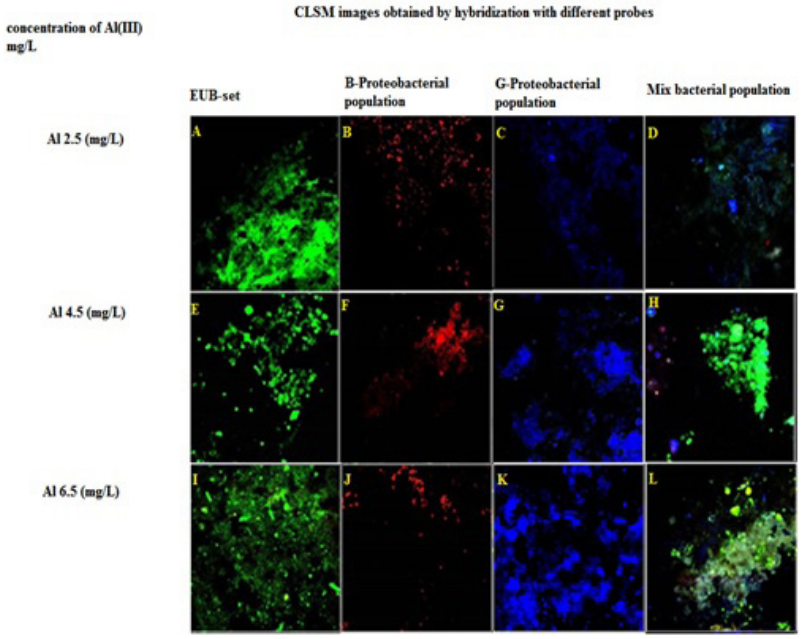

Fig. 6. CLSM of biofilm, at 10x, developed on tire rubber surface taken from AGBR dosed with Al^{3+} (2.5, 4.5, 6.5 mg/L, respectively). (A) EUB mixture of probes depicting the population of eubacteria. (B) β-42+unlabeled competitor probe depicting β-proteobacterial population. (C) γ-42 probe+ competitive inhibitor depicting the γ-proteobacteria as blue fluorescing cells. (D) Mixed probes hybridized simultaneously. CLSM of biofilms at Al^{3+} (4.5 mg/L). (E) EUB mixture of probes depicting the general population. (F) β-42 + unlabeled competitor probe depicting β-proteobacterial population. (G) γ-42 probe+competitive inhibitor depicting the γ-proteobacteria as blue fluorescing cells. (H) Mixed probes hybridized simultaneously. CLSM of biofilm, at Al^{3+} (6.5 mg/L). (I) EUB mixture of probes depicting the general population. (J) β-42+unlabeled competitor probe. (K) γ-42 probe+competitive inhibitor. (L) Mixed probes hybridized simultaneously, overlap of probes produces secondary color fluorescence. In figure: G, gamma, B, beta.

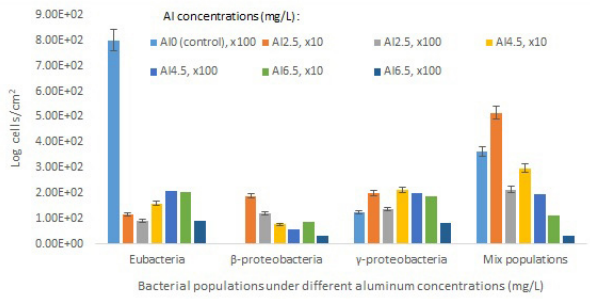

Fig. 7. Bacterial population count, quantified using DAIME software, for the biofilms developed under varying concentrations of Al^{3+} (0, 4.5, 6.5 mg/L). Carboxyfluorescein (FAM)-labeled probes targeting Eubacterial, β-proteobacterial and γ-proteobacterial population were used for individual sections of the biofilm from tire-derived rubber support and viewed under confocal laser scanning microscopy.

and 9.00E+01 at 4.5, 6.5 and 2.5 mg/L of Al^{3+}, respectively. Conversely, the population of gamma and beta-Proteobacteria decreased with increasing concentration of Al^{3+} (mg/L).

At 100x, the population of γ-proteobacteria (object count 1.35 E+02) was greater than β-proteobacteria (object count 1.19E+02). Similarly, for the biofilm developed on tire-derived rubber at 4.5 mg/L Al^{3+} (mg/L) the approximate object counts of β- and γ-proteobacteria were 7.60E+01 and 2.12E+02, respectively. The same trend, that is, the dominance of γ-proteobacteria over β-proteobacteria was observed in the FOV taken at 100x magnification, with an average count of 5.60E+01 and 2.01E+02, respectively. Biofilm sample taken from tire rubber treated with 6.5 mg/L Al^{3+} gave higher object count (8.00E+01) for γ-proteobacteria than β-proteobacteria (3.00E+01) at 100x magnification.

4. Discussion

The unmitigated growth of biofilms over surfaces in potable water and sanitary systems has been presented as a nuisance factor leading toward microbially induced corrosion [33,34], contamination of eatables and associated problems [35–38]. Simultaneously, biofilms functioning as catalytic matrices on attached growth reactors have been viewed as being vital for possible biodegradation and biotransformation of water contaminants specifically of soluble nature [39,40]. Biofilms matrix in wastewater treatment systems and their interaction with heavy metals have been reported previously [41,15]. The role of Al^{3+} in ground water has been established as an important coagulant for removal of organic and inorganic matter [42,22]. However, its role in biofilm development particularly on diversity of potential bacteria with regards to waste water technology has not been studied extensively compared with other metal elements. The study comprehensively established the limiting effects of narrow range (2.5–6.5 mg/L) of aluminum concentrations on the density and diversity of bacteria on TDR biofilms in AGBR. Gamma proteobacteria compared with beta-proteobacteria dominated the overall proteobacterial population. Additionally, the residual amount of aluminum proved to be affecting the sludge digestibility and related performance of the reactor.

The presence of Al^{3+} (mg/L) in the aqueous environment has been associated with mitigation of biofilm development on support surfaces and bacterial physiological processes such as porphyrin metabolism [39,43], DNA chelation, [44,45] and intracellular accumulation due to siderophores production [46,47]. Transmission electron microscopy (TEM) and SYTOX staining conducted by Yaganza et al. [48] revealed that $AlCl_3$ loosened the cell wall, subsequently causing leakage and rupturing of bacterial cells, and nucleic acid complexation when exposure time was lengthened. Though these transformations were marked at higher concentration (0.2 M) of Al^{3+}, they were also reported at lower concentrations (0.05 M and 0.1 M). Besides, it was also established that toxicity was not influenced by pH but was primarily due to Al^{3+}. Therefore, considering the occurrence of an almost neutral pH in the AGBR it can be clearly deduced that increasing Al^{3+} concentration (mg/L) only placed a metabolic stress on microbial population. The mechanism of toxicity of aluminum ions has been attributed to the nature of Al^{3+} ions as low charged complex acid $[Al(H_2O)_6]_3$ ion, in aqueous environment. As indicated by cytoplasmic accretion these acidic complexes reported to be diffusing in to the cell by disrupting the cell wall and forming complexes with catalytic subunits and nucleic acids [49–51]. In addition, Gossett et al. [52] in their study on the negative effects of metal coagulants revealed that there was a substantial decrease in volatile solids destruction, methane production, COD removal, organic nitrogen catabolism and alkalinity production. The underlying mechanisms causing the aforementioned problems was attributed to the phenomenon of coagulants "locking up" substrates such as proteins [53] or phosphate limitation caused by aluminum and iron precipitation of phosphorus.

Bacterial densities on TDR biofilm revealed by FISH-CLSM (Fig. 7) were complimentary to ones obtained through conventional culture based bacterial counting (CFU/mL cm^2) method. Moving across the concentration gradients, inhibitory effect of increasing Al^{3+} concentration (mg/L) were reflected in the spatial distribution of gamma- and beta-proteobacteria. The increase in Al^{3+} concentration (mg/L) led to an overall decrease in the gamma and beta-proteobacterial populations. Furthermore, the ratio of gamma-proteobacteria on tire rubber for all concentrations was greater than β-proteobacterial population (Fig. 5), with highest number of bacteria from both phyla in 2.5 mg/L, followed by 4.5 mg/L and then 6.5 mg/L of Al^{3+}. Similarly, bacterial profiling based on CLSM and molecular characterization conducted by Lin [54], on different piping surfaces coupons indicated that for stainless steel, PVC, and cast iron the ratio of gamma-proteobacteria was significantly greater than β-proteobacteria. Similarly, Desai et al. [55] reported predominance of gamma-proteobacteria over beta-proteobacteria on highly contaminated chromium soil. Furthermore, predominance of gamma-proteobacteria was reported by Sun et al. [56] in the two 16S rDNA clone libraries they had constructed of the endophytic bacterial community isolated from copper resistant plants grown on copper contaminated soil.

Previously different fixed film reactors demonstrated establishment of bacterial biofilms [9]. Although various physical and chemical factors proved to be effecting bacterial growth [57,58], Vukanti et al. [59] in their study on tire rubber crumb in landfills isolated culturable aerobic and anaerobic

bacteria that included *Bacillus megaterium*, *Bacillus pumilus*, *Bacillus cereus*, *Arthrobacter globiformis*, *Flavobacterium* sp., *Clostridium* sp., *Enterobacter aerogenes, Enterococcus faecium* and *Cellulosimicrobium cellulans.* Nevertheless, microbicidal products such as accelerators, antioxidants and vulcanizing agents proved to be inhibitory for certain bacteria while other constituents of tire rubber exerted positive influence on biofilm formation [60]. In this context, Zn^{2+}in tire rubber has been reported specifically for development of biofilm by *Salmonella enterica* subsp. *Enterica* serovar *Typhimurium* [61].

Since, activated sludge was used as a seed, biochemical characterization of bacterial isolates demonstrated presence of species of *Enterobacter*, *Pseudomonas*, *Serratia*, *Klebsiella*, *Salmonella*, *Proteus*, *Bacillus*, *Staphylococcus*, *Shigella*, *Citrobacter* and *E. coli* (Table S4). Likewise, members of *Enterobacteriaceae* including *Aeromonas*, *Campylobacter*, *Pseudomonas*, *Salmonella*, and *Helicobacter* have been reported in biofilms developed on plastic and metallic piping materials [35,62–64]. September et al. [65] in their study reported the incidence of *Pseudomonas*, *Shigella*, *E. coli*, *Salmonella* and *Vibrio* spp. within biofilm samples that were isolated from drinking water supply pipelines in South Africa.

Biological reactors containing tire-derived rubber as support materials have also been found considerably effective in treatment of wastewater. Barros et al. [66] compared the efficacy of two anaerobic fluidized bioreactors (AFBR) that used different support materials including polyethylene and tire rubber. According to their findings, tire rubber AFBR showed better performance possibly due to better biofilm development on it. Besides, physical features of tire rubber might have provided crevices; shielding biofilms colonization [66]. Minor amount of aluminum, that is, 2.5 mg/L proved to be important regarding percentage change of NO_2^- in the sludge whereas, further decrease or increase in aluminum proved to be considerably limiting (Fig. 3). Decrease in NO_3-N, in aerobic trickling filters, has been previously associated with presence of anammox bacteria in the reactor [67] as these facilitate complete ammonia removal and denitrification of nitrite with ammonia as the electron donor [68], via autotrophic pathways without the requirement for organic carbon. The highest removal of COD at lower concentration (2.5 mg/L) Al^{3+}might be due to higher contribution of heterotrophic bacteria in denitrification of nitrogenous compounds [69]. VFA and alkalinity of the AGBR showed an inverse relationship with each other in sludge digestion. Increase in aluminum resulted in a decrease in alkalinity with a simultaneous increase in case of VFA (Fig. 2). Study by Lin [54] on the effect of heavy metals such as Cd, Cu, Zn, Pb and Cr on VFA production in an anaerobic digester showed that higher concentrations of Pb, Zn and Cd increased the production of VFA by 160%–700%. Further, reports have mentioned stimulating effect on VFAs production by the addition of Ni and Zn. Nevertheless limiting effect on VFAs production was observed with Cu and Pb. The rational for the increase in VFA concentration with increasing concentration for certain metal ions has not been well elucidated. However, it is imperative to recall that VFA production is due to acidogenic bacteria converting organic acid into short chain fatty acids, making them more resistant to environmental stresses. So, it can be hypothesized that these organic acids bind to $Al^{3+}$and inhibit its toxic effect [70]. The activity differences with increasing Al^{3+} concentrations might be due to the stress exerted by Al^{3+} mg/L on the metabolic pathway of heterotrophic bacteria [49].

5. Conclusion

Tire-derived rubber supported a high diversity of bacteria and proved to be a suitable support material for developing biofilms in attached growth bioreactors. Simultaneous use of aluminum as a coagulant proved to be limiting sludge digestibility and AGBR performance. Conventional and molecular studies consolidated the fact that increasing aluminum concentrations under batch conditions have a limiting effect, though non-significant, on bacterial density as well as diversity. Therefore, a wider range of Al^{3+} (mg/L) concentration must be studied in order to find out the positive impacts on sludge stability and associated digestion with effective indigenous microbial consortium.

Acknowledgments

The authors would like to specially thank Dr. Qaiser Mahmood Khan and his colleagues from Environmental Biotechnology Division, National Institute of Biotechnology and Genetic Engineering (NIBGE), Faisalabad, Pakistan, for facilitating and providing invaluable guidance in performing FISH and sharing the use of their confocal lasing scanning microscope, for our research.

References

[1] T. Todhanakasem, Developing microbial biofilm as a robust biocatalyst and its challenges, Biocatal. Biotransform., 35 (2017) 86–95.
[2] T. Yoshizawa, M. Miyahara, A. Kouzuma, K. Watanabe, Conversion of activated-sludge reactors to microbial fuel cells for wastewater treatment coupled to electricity generation, J. Biosci. Bioeng., 118 (2014) 533–539.
[3] M. Katsikogianni, Y.F. Missirlis, Concise review of mechanisms of bacterial adhesion to biomaterials and of techniques used in estimating bacteria-material interactions, Eur. Cell. Mater., 8 (2004) 37–57.
[4] H.H. Tuson, D.B. Weibel, Bacteria–surface interactions, Soft Matter, 9 (2013) 4368.
[5] M.Yikmis, A. Steinbüchel, Historical and recent achievements in the field of microbial degradation of natural and synthetic rubber, Appl. Environ. Microbiol., 78 (2012) 4543–4551.
[6] Z. Tang, M.A. Butkus, Y.F. Xie, Crumb rubber filtration: a potential technology for ballast water treatment, Mar. Environ. Res., 61 (2006) 410–423.
[7] J. Park, T.G. Ellis, M. Lally, Evaluation of Tire Derived Rubber Particles for Biofiltration Media, Proc. Water Environment Federation WEFTEC, 2006, pp. 3217–3230.
[8] J. Park, Evaluation of Tire Derived Rubber Particles as Biofilter Media and Scale-up and Design Considerations for the Static Granular Bed Reactor (SGBR), Retrospective Theses and Dissertations, Lowa, 2008.
[9] I. Naz, N. Khatoon, I. Ali, D.P. Saroj, S.A. Batool, S. Ahmed, Appraisal of the tire derived rubber (TDR) medium for wastewater treatment under aerobic and anaerobic conditions, J. Chem. Technol. Biotechnol., 89 (2013) 587–596.
[10] T. González, J.R. Domínguez, J.B. Heredia, H.M. García, F.S. Lavado, Aluminium sulfate as coagulant for highly polluted cork processing wastewater: evaluation of settleability parameters and design of a clarifier-thickener unit, J. Hazard. Mater., 148 (2007) 6–14.
[11] G. Zhu, H. Zheng, W. Chen, W. Fan, P. Zhang, T. Tshukudu, Preparation of a composite coagulant: polymeric aluminum

ferric sulfate (PAFS) for wastewater treatment, Desalination, 285 (2012) 315–323.
[12] B. Vu, M. Chen, R.J. Crawford, E.P. Ivanova, Bacterial extracellular polysaccharides involved in biofilm formation, Molecules, 14 (2009) 2535–2554.
[13] M.I. Samanovic, C. Ding, D.J. Thiele, K.H. Darwin, Copper in microbial pathogenesis: meddling with the metal, Cell Host Microbe, 11 (2012) 106–115.
[14] L. Nan, K. Yang, G. Ren, Anti-biofilm formation of a novel stainless steel against *Staphylococcus aureus*, Mater. Sci. Eng. C, 15 (2015) 356–361.
[15] G.M. Teitzel, M.R. Parsek, Heavy metal resistance of biofilm and planktonic *Pseudomonas aeruginosa*, Appl. Environ. Microbiol., 69 (2003) 2313–2320.
[16] I. Douterelo, J.B. Boxall, P. Deines, R. Sekar, K.E. Fish, C.A. Biggs, Methodological approaches for studying the microbial ecology of drinking water distribution systems, Water Res., 65 (2014) 134–156.
[17] T.R. Neu, J.R. Lawrence, Investigation of microbial biofilm structure by laser scanning microscopy, Productive Biofilms, 146 (2014) 1–51.
[18] M. Herten, T. Bisdas, D. Knaack, K. Becker, N. Osada, G.B. Torsello, E.A. Idelevich, Rapid in vitro quantification of *S. aureus* biofilms on vascular graft surfaces, Front. Microbiol., 8 (2017) 23–33.
[19] K.E. Fish, R. Collins, N.H. Green, R.L. Sharpe, I. Douterelo, A.M. Osborn, J.B. Boxall, Characterisation of the physical composition and microbial community structure of biofilms within a model full-scale drinking water distribution system, PLoS One, 10 (2015) 1–22.
[20] I. Sharafat, D.K. Saeed, S. Yasmin, A. Imran, Z. Zafar, A. Hameed, N. Ali, Interactive effect of trivalent iron on activated sludge digestion and biofilm structure in attached growth reactor of waste tire rubber, Environ. Technol., 39 (2018) 130–143.
[21] C. Park, Y. Fang, S.N. Murthy, J.T. Novak, Effects of floc aluminum on activated sludge characteristics and removal of 17-ethinylestradiol in wastewater systems, Water Res., 44 (2010) 1335–1340.
[22] C. Park, C.D. Muller, M.M. Abu-Orf, J.T. Novak, The Effect of wastewater cations on activated sludge characteristics: effects of aluminum and iron in floc, Water Environ. Res., 78 (2006) 31–40.
[23] S.N. Murthy, J.T. Novak, Influence of cations on activated-sludge effluent quality, Water Environ. Res., 73 (2001) 30–36.
[24] Anne, R. Evans, The Composition of a Tyre: Typical Components 5. Oxen. The Waste & Resources Action Programme, Oxen, 2006.
[25] K. Buchauer, A comparison of two simple titration procedures to determine volatile fatty acids in influents to waste-water and sludge treatment processes, Water SA, 24 (1998) 49–56.
[26] M.A.H. Franson, Standard Methods for the Examination of Water and Wastewater, American Public Health Association, Washington D.C., USA, 2005.
[27] J.H. Holt, N.R. Krieg, P.H. Sneath, J.T. Staley, S.T. Williams, Bergey's Manual of Determinative Bacteriology, 9th ed., Eur. J. Paediatr. Neurol., 13 (1994) 560.
[28] W. Manz, K.W. Potthoff, T.R. Neu, U. Szewzyk, J.R. Lawrence, Phylogenetic composition, spatial structure, and dynamics of lotic bacterial biofilms investigated by fluorescent in situ hybridization and confocal laser scanning microscopy, Microb. Ecol., 37 (1999) 225–237.
[29] H. Daims, S. Lücker, M.D.Wagner, A novel image analysis program for microbial ecology and biofilm research, Environ. Microbiol., 8 (2006) 200–213.
[30] R.I. Amann, B.J. Binder, R.J. Olson, S.W. Chisholm, R. Devereux, D.A. Stahl, Combination of 16S rRNA-targeted oligonucleotide probes with flow cytometry for analyzing mixed microbial populations, Appl. Environ. Microbiol., 56 (1990) 1919–1925.
[31] E.W. Alm, D.B. Oerther, N. Larsen, The oligonucleotide probe database, 62 (1996) 3557–3559.
[32] J. Brosius, T.J. Dull, D.D. Sleeter, H.F. Noller, Gene organization and primary structure of a ribosomal RNA operon from *Escherichia coli*, J. Mol. Biol., 148 (1981) 107–127.
[33] I.B. Beech, J.A. Sunner, K. Hiraoka, Microbe-surface interactions in biofouling and biocorrosion processes, Int. Microbiol., 8 (2005) 157–168.
[34] J. Mansouri, S. Harrisson, V. Chen, Strategies for controlling biofouling in membrane filtration systems: challenges and opportunities, J. Mater. Chem., 20 (2010) 45–67.
[35] A. Dufour, M. Snozzi, W. Koster, J. Bartram, E. Ronchi, L. Fewtrell, Assessing Microbial Safety of Drinking Water, International Water Association Publishing, London, UK, 2003.
[36] P. Borella, E. Guerrieri, I. Marchesi, M. Bondi, P. Messi, Water ecology of *Legionella* and protozoan: environmental and public health perspectives, Biotechnol. Annu. Rev., 11 (2005) 355–380.
[37] J.D. Brooks, S.H. Flint, Biofilms in the food industry: problems and potential solutions, Int. J. Food Sci. Technol., 43 (2008) 2163–2176.
[38] X. Shi, X. Zhu, Biofilm formation and food safety in food industries, Trends Food Sci. Technol., 20 (2009) 407–413.
[39] D. Domaradzka, U. Guzik, D. Wojcieszyńska, Biodegradation and biotransformation of polycyclic non-steroidal anti-inflammatory drugs, Rev. Environ. Sci. Biotechnol., 14 (2015) 229–239.
[40] R.G. Saratale, G.D. Saratale, J.S. Chang, S.P. Govindwar, Decolorization and biodegradation of reactive dyes and dye wastewater by a developed bacterial consortium, Biodegradation, 21 (2010) 999–1015.
[41] S. Koechler, J. Farasin, J. Cleiss-Arnold, F. Arsène-Ploetze, Toxic metal resistance in biofilms: diversity of microbial responses and their evolution, Res. Microbiol., 166 (2015) 764–773.
[42] H.K. Shon, S. Vigneswaran, I.S. Kim, J. Cho, H.H. Ngo, The effect of pretreatment to ultrafiltration of biologically treated sewage effluent: a detailed effluent organic matter (EfOM) characterization, Water Res., 38 (2004) 1933–1939.
[43] R. Scharf, R. Mamet, Y. Zimmels, S. Kimchie, N. Schoenfeld, Evidence for the interference of aluminum with bacterial porphyrin biosynthesis, Biometals, 7 (1994) 135–141.
[44] L. Guida, Z. Saidi, M.N. Hughes, R.K. Poole, Aluminium toxicity and binding to *Escherichia coli*, Arch Microbiol., 156 (1991) 507–512.
[45] J. Guzzo, A. Guzzo, M.S. DuBow, Characterization of the effects of aluminum on luciferase biosensors for the detection of ecotoxicity, Toxicol. Lett., 64-65 (1992) 687–693.
[46] M.M.D. Carvalho, D.G. Edwards, C.J. Asher, C.S. Andrew, Effects of aluminium on nodulation of two Stylosanthes species grown in nutrient solution, Plant Soil, 64 (1982) 141–152.
[47] S. Silver, M. Walderhaug, Gene Regulation of plasmid- and chromosome-determined inorganic ion transport in bacteria, Microbiol. Rev., 56 (1992) 195–228.
[48] E.S. Yaganza, D. Rioux, M. Simard, J. Arul, R.J. Tweddell, Ultrastructural alterations of *Erwinia carotovora* subsp. *atroseptica* caused by treatment with aluminum chloride and sodium metabisulfite, Appl. Environ. Microbiol., 70 (2004) 6800–6808.
[49] A.C. Johnson, M. Wood, DNA, A possible site of action of aluminum in *Rhizobium* spp., Appl. Environ. Microbiol., 15 (1990) 3629–3633.
[50] M. Wood, A mechanism of aluminium toxicity to soil bacteria and possible ecological implications, Plant Soil, 171 (1995) 63–69.
[51] T.P. Mossor, Effect of aluminium on plant growth and metabolism, Acta Biochim. Pol., 48 (2001) 673–686.
[52] J.M. Gossett, P.L. McCarty, J.C. Wilson, D.S. Evans, Anaerobic digestion of sludge from chemical treatment, J. Water Pollut. Control Fed., 50 (1978) 533–542.
[53] W. Rudolfs, L.R. Setter, After-effect of Ferric Chloride on sludge digestion, Sewage Works J., 3 (1931) 352–361.
[54] C.Y. Lin, Effect of heavy metals on acidogenesis in anaerobic digestion, Water Res., 27 (1993) 147–152.
[55] C. Desai, R.Y. Parikh, T. Vaishnav, Y.S. Shouche, D. Madamwar, Tracking the influence of long-term chromium pollution on soil bacterial community structures by comparative analyses of 16S rRNA gene phylotypes, Res. Microbiol., 160 (2009) 1–9.
[56] L.N. Sun, Y.F. Zhang, L.Y. He, Genetic diversity and characterization of heavy metal-resistant-endophytic bacteria from two copper-tolerant plant species on copper mine wasteland, Bioresour Technol., 101 (2010) 501–509.

[57] M.M. Berekaa, A. Linos, R. Reichelt, U. Keller, A. Steinbüchel, Effect of pretreatment of rubber material on its biodegradability by various rubber degrading bacteria, FEMS Microbiol Lett., 184 (2000) 199–206.
[58] P.J. Sheehan, J.M. Warmerdam, S. Ogle, D.N. Humphrey, S.M. Patenaude, Evaluating the risk to aquatic ecosystems posed by leachate from tire shred fill in roads using toxicity tests, toxicity identification evaluations, and groundwater modeling, Environ. Toxicol. Chem., 25 (2006) 400–411.
[59] R. Vukanti, M. Crissman, L.G. Leff, A.A. Leff, Bacterial communities of tyre monofill sites : growth on tyre shreds and leachate, J. Appl. Microbiol., 106 (2009) 1957–1966.
[60] M. Christiansson, B. Stenberg, O. Holst, Toxic additives - a problem for microbial waste rubber desulphurisation, Resour. Environ. Biotechnol., 3 (2000) 11–21.
[61] M. Crampton, A. Ryan, C. Eckert, K.H. Baker, D.S. Herson, Effects of leachate from crumb rubber and zinc in green roofs on the survival, growth, and resistance characteristics of *Salmonella enterica* subsp. *enterica* serovar *Typhimurium*, Appl. Environ. Microbiol., 80 (2014) 2804–2810.
[62] U. Szewzyk, R. Szewzyk, W. Manz, K.H. Schleifer, Microbiological safety of drinking water, Annu. Rev. Microbiol., 58 (2000) 81–127.
[63] P.R. Hunter, J.M. Colford, M.W. LeChevallier, S. Binder, P.S. Berger, Panel on Waterborne Diseases, Emerg. Infect. Dis., 58 (2001) 544–544.
[64] D.G. Lee, S.J. Kim, Bacterial species in biofilm cultivated from the end of the Seoul water distribution system, J. Appl. Microbiol., 95 (2003) 317–324.
[65] S.M. September, F.A. Els, S.N. Venter, V.S. Brözel, Prevalence of bacterial pathogens in biofilms of drinking water distribution systems, J. Water Health, 5 (2007) 219–227.
[66] A.R. Barros, E.L.C.D. Amorim, C.M. Reis, G.M. Shida, E.L. Silva, Biohydrogen production in anaerobic fluidized bed reactors: effect of support material and hydraulic retention time, Int. J. Hydrogen Energy, 35 (2010) 3379–3388.
[67] J. Wilsenach, L. Burke, V. Radebe, Anaerobic ammonium oxidation in the old trickling filters at Daspoort Wastewater Treatment Works, Water SA. 40 (2014) 81–88.
[68] V. Loosdrecht, Jetten, Method of Treating Ammonia-Comprising Waste Water, European Patent Office, Delft, 1998.
[69] Q. Xiangli, Z. Zhenjia, C. Qingxuan, C. Yajie, Nitrification characteristics of PEG immobilized activated sludge at high ammonia and COD loading rates, Desalination, 222 (2008) 340–347.
[70] D.L. Jones, A.M. Prabowo, L.V. Kochian, Kinetics of malate transport and decomposition in acid soils and isolated bacterial populations: the effect of microorganisms on root exudation of malate under Al stress, Plant Soil, 182 (1996) 239–247.

Supplementary material

Table S1
Characteristics of treated activated sludge as COD, volatile fatty acid and alkalinity in AGBR after 30 d of treatment

S. No.	VFA (mg/L)	Alkalinity	COD (mg/L)
Control	147.6	7.54	509
2.5	227.67	6.25	363
4.5	250.03	4.9	371
6.5	350	2.5	438

Note: Characteristics of raw sludge before treatment: COD, 700 mg/L, VFA, 27.5 mg/L, Alkalinity, 9.5.

Table S2
Transformation rate of nitrogen in terms of NO_2^- (A) and NO_3^-(B) in the activated sludge treated at different concentrations of Al^{3+}

Sample	Week	Week	Week	A	B	% A	% B
	1	2	3	0	0	Decrease	Decrease
Concentration of nitrites (mg/L)							
Control	182	74	44	10.8	13.8	59.34	73.4
Al - 2.5	39	96	66	2.7	3	59.3	76.92
Al - 4.5	47	45	43	2	4	40	8.5
Al - 6.5	59	71	46	12[a]	13	20.33[a]	22.03%
Concentration of nitrates (mg/L)							
Control	168.8	206.6	163.7	37.8	18.35	22.39[a]	30.2
Al - 2.5	219.7	170.5	148.4	49.2	7.13	22.39	32.45
Al - 4.5	249.2	118.1	114.2	13.11	52.6	52.6	54.17
Al - 6.5	216.1	172.6	115.8	4.34	10.03	20.09	46.41

[a]% Increase.

Table S3
CFU/mL/cm^2 at varying concentrations of Al^{3+} mg/L at different dilutions

Dilutions	CFU/mL/cm^2			
	10^4	10^5	10^6	10^7
Concentration of Al^{3+} (mg/L)				
0	6.16×10^7	4.52×10^8	4.20×10^9	3.15×10^{10}
2.5	1.19×10^7	2.80×10^7	6.30×10^8	2.50×10^9
4.5	6.70×10^6	3.00×10^8	1.50×10^8	3.00×10^8
6.5	4.60×10^6	2.10×10^7	9.00×10^7	4.00×10^8

Table S4
Biochemical observations of different bacterial isolates from TDR biofilm in the AGBR

Isolate no.	TSI			MR	VP	SIM			Urease	Catalase	Oxidase	Nit	Citrate	Potential bacterial species
	Slant/ butt	H_2S	Gas			Mot	Ind	Bubble						
1	K/A	–	–	–	+	+	–	–	+	+	–	+	+	*Serratia*
2	K/A	–	–	–	+	–	–	–	–	+	+	+	+	*Enterobacter*
3	K/K	–	–	+	–	–	–	+	–	+	+	+	+	*Pseudomonas*
4	K/K	–	–	–	–	–	–	–	±	+	–	+	+	*Proteus*
5	A/K	–	–	–	–	+	+	–	±	+	+	+	+	*Citrobacter*
6	K/A	–	–	–	–	+	–	–	±	+	+	+	+	*Enterobacter aerogenes*
7	K/A	–	–	–	+	+	–	–	–	+	+	+	+	*Bacillus*
8	K/A	–	–	–	–	+	–	–	–	+	–	+	–	*Klebsiella pneumonia*
9	K/A	–	–	–	+	+	–	+	–	+	+	+	+	*Klebsiella/Erwinia*
10	K/K	–	–	–	–	+	–	–	–	+	+	+	+	*Salmonella*
11	A/A	–	+	+	–	+	+	–	–	+	–	+	–	*Escherichia coli*
12	K/A	–	–			–	–			+	+	+	–	*Staphylococcus*
13	A/K	–	+	–	–	+	–	–	–	+	+	+	–	*Shigella*
14	K/A	–	–	+	–	+	–	–	–	+	+	+	+	*Staphylococcus*
15	A/K	–	–	–	+	+	–	–	±	–	+	+	–	*Bacillus megaterium*

H_2S, hydrogen sulfide production test; MR, methyl red test; VP, Voges–Proskauer test; Nit, nitrate reduction test; Ind, indole test; Mot, motility test; K, Alkaline; A, Acidic.

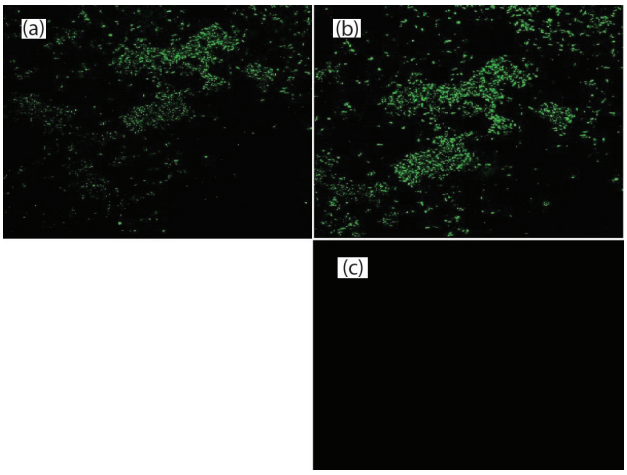

Fig. S1. Pure culture of *Pseudomonas* fixed on three teflon coated wells of the slide to test the specificity of probes. (a) Fluorescens due to hybridization with EUB-mix pobe set (EUB I, II and III) probes. (b) Hybridization with G-42 probes also produces flourescens. (c) No flourescens produced with B-42 probes establishing specificity of the probes with only the G-proteobacterial population.

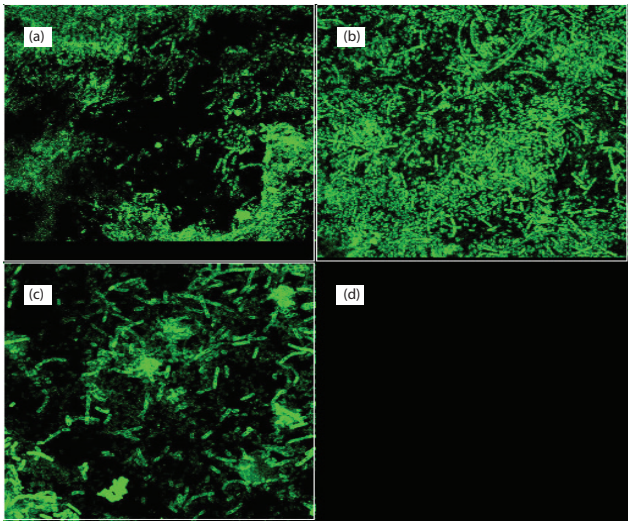

Fig. S2. Pure culture of Bacillus fixed on four wells of the slide. (a) Fluorescens due to hybridization with EUB-mix pobe set (EUB I, II and III) probes. (b) Hybridization with beta probes also produces flourescens. (c) No flourescens produced with gamma probes establishing specificity of the probes with only the B-population. (d) Flouresing green rods depicting bacilli when mixture of probes; EUB probe set+beta probes along with the beta probe competitors were used.